Use of Parabolic Sections to Shape the Main Reflector of Omnidirectional Dual-Reflector Antennas

R. A. Penchel[1], S. R. Zang[1], J. R. Bergmann[1] and F. J. S. Moreira[2]

Abstract – **This work presents a formulation for shaping the main reflector of an axis-symmetric dual reflector antenna designed to offer an omnidirectional coverage with an arbitrary radiation pattern in the vertical plane. The subreflector surface is generated by a hyperbola while the shaped main reflector is generated by a series of local parabolic sections sequentially concatenated. As case studies, two representative axis-displaced Cassegrainian configurations are synthesized to radiate, under GO principles, a cosecant radiation pattern in the elevation plane. For a rigorous antenna analysis, a hybrid technique based on Mode Matching and Method of Moments is employed.**

1 INTRODUCTION

This work investigates the main-reflector synthesis for omnidirectional dual-reflector antennas. The body-of-revolution subreflector is generated by a single conic section (a hyperbola, in the present study) while the shaped main reflector is generated by a series of local parabolic sections (see Fig. 1). The shaping of dual-reflector antennas based on the combination of local conic sections has been already investigated [1]. The concepts were further improved to treat arbitrary axisymmetric dual-reflector configurations [2] and omnidirectional dual-reflector arrangements [3]. Furthermore, the studies presented in [4], [5], and [6] have been extended to design omnidirectional axis-displaced Cassegrain (OADC) and Ellipse (OADE) antennas, where only the main reflector was shaped to provide constant sectorial coverage in the elevation plane. Differently from [1]–[6], in the present design procedure parabolas are used instead of ellipses or hyperbolas to locally describe the shaped main-reflector generatrix. The procedure is simpler than that based on conic sections.

2 SYNTHESIS AND ANALYSIS METHOD

In the present shaping technique, the main reflector generatrix is described by a combination of N local parabolic sections M_n sequentially concatenated, all of them with their focci at a common point P (see Fig. 1). Each parabolic section M_n is limited by angles θ_{Sn-1} and θ_{Sn} and its axis passes through P and makes an angle γ_n with the z-direction. The distance r_S between P and a point at M_n and is given by:

$$r_S = \frac{2\,F_n}{[\cos(\gamma_n - \theta_S) - 1]}, \text{for } \theta_S \in [\theta_{Sn-1}, \theta_{Sn}] \qquad (1)$$

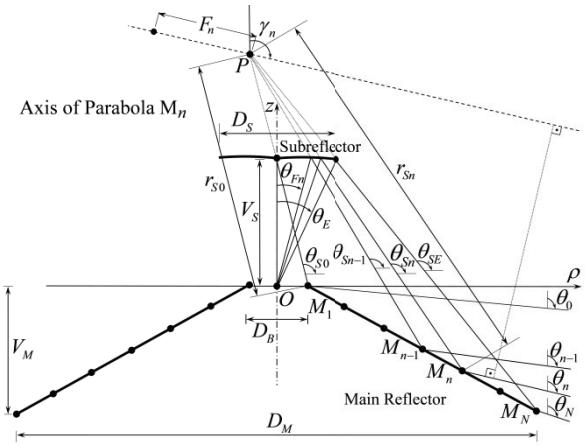

Fig. 1 – Parabolic conic sections representing the shaped generatrix of the main reflector.

Two parameters must be determined for each section M_n: the focal distance F_n and the parabola axial tilt γ_n. To accomplish that, the mapping relation between the feed ray direction θ_F and the subreflector ray direction θ_S will be useful [7]:

$$\cot\left(\frac{\theta_S}{2}\right) = \frac{\varepsilon\cos\beta + 1 - \varepsilon\sin\beta\cot(\theta_F/2)}{\varepsilon\sin\beta + (\varepsilon\cos\beta - 1)\cot(\theta_F/2)} \qquad (2)$$

where ε is the eccentricity and β is the axial tilt angle of the hyperbola that generates the subreflector.

In the numerical procedure for an OADC configuration, the feed angle θ_F is increasingly varied from 0 to θ_E, with $\theta_{Fn} - \theta_{Fn-1} = \Delta\theta_F = \theta_E/N$. The initial parameters ($n = 0$) are determined by the locations of the subreflector edge and of the main-reflector central opening, located by the parameters V_S, z_B, D_S, D_B, and θ_E previously used to specify the subreflector. For $n = 1,\ldots, N$, the parabola M_n is determined as follows. From (1) and the values of r_{Sn-1} and θ_{Sn-1} determined in the previous step (n–1) one obtains:

$$F_n = \frac{r_{Sn-1}}{2}[\cos(\gamma_n - \theta_{Sn-1}) - 1] \qquad (3)$$

Applying the conservation of energy to the tube of rays departing from O, one obtains a relation between θ_{Fn} and γ_n:

$$\int_0^{\theta_{Fn}} G_F(\theta_F)\sin\theta_F \mathrm{d}\theta_F = N_F \int_{\theta_0}^{\gamma_n} G_A(\theta)\sin\theta \mathrm{d}\theta \qquad (4)$$

[1] CETUC, Pontifical Catholic University of Rio de Janeiro, Rio de Janeiro, RJ, Brazil, 22451-900,
e-mail: { rapenchel, sandro, bergmann }@cetuc.puc-rio.br
[2] DELT, Federal University of Minas Gerais, Belo Horizonte, MG, Brazil, 31270-901,
e-mail: fernandomoreira@ufmg.br

978-1-4673-5707-4/13/$31.00 ©2013 IEEE

where $G_F(\theta_F)$ is the feed circularly symmetric radiation pattern, $G_A(\theta)$ the prescribed vertical GO pattern in the far-field region of the main reflector and N_F is normalization constant to ensure that the power inside the tube of rays remains constant. Once F_n and γ_n are obtained, r_{Sn} is calculated for further use in the following step (n+1):

$$r_{Sn} = \frac{2\,F_n}{[\cos(\gamma_n - \theta_{Sn}) - 1]} \tag{5}$$

The procedure is very simple and yields a continuous generatrix, but with discontinuous derivative at points shared by adjacent parabolas.

To ensure vertical polarization, the dual-reflector antenna designs can be fed by a coaxial TEM horn, illustrated in Fig. 2. In order to estimate the electromagnetic performance of the antenna, a rigorous analysis is employed. The method combines the Mode Matching Technique (MMT) to treat the fields inside of the feed coaxial TEM horn, which is represented as series of stepped coaxial waveguide sections (Fig. 3.a), and the Method of Moments (MoM) to solve a combination of electric and magnetic field integral equations to calculate the exterior equivalent surface currents (Fig. 3.b) and, consequently, the amplitudes $[b^A]$ of the modes reflected back into the horn [8], [9].

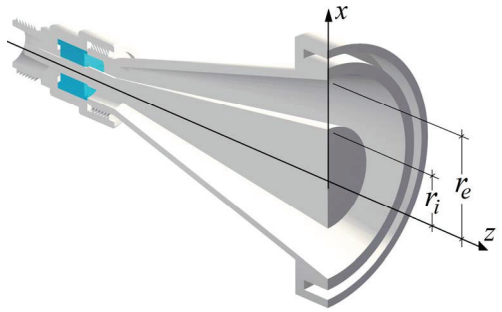

Fig. 2 – Coaxial TEM horn.

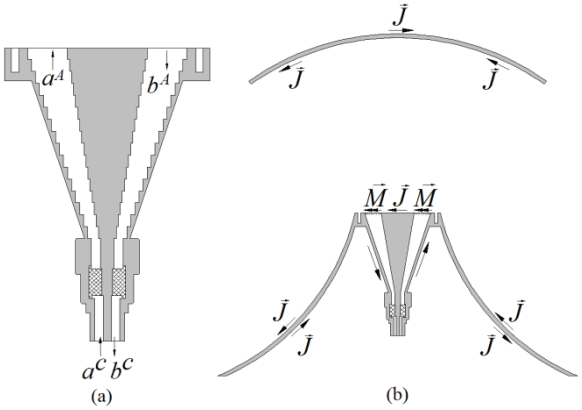

Fig. 3 – (a) Coaxial horn represented as series of stepped waveguides and (b) MoM model of the exterior surface currents (feed and reflectors).

3 CASE STUDIES

To evaluate the proposed shaping procedure, the main reflector was shaped to generate a cosecant squared radiation pattern $G_A(\theta)$ in elevation plane, described by:

$$G_A(\theta) = G_{Ao}\csc^2(\theta - \pi/2)\,, \quad \text{for } \theta \in [\theta_0, \theta_N] \tag{6}$$

where G_{Ao} is a normalization factor [7]. The function that describes the feed radiation pattern in the far-field region is given by:

$$G_F(\theta_F) = G_{Fo}\left[\frac{\mathrm{J}_0(kr_i \sin\theta_F) - \mathrm{J}_0(kr_e \sin\theta_F)}{\sin\theta_F}\right]^2 \tag{7}$$

where G_{Fo} is a normalization factor. Equation (7) represents the radiation from a coaxial aperture on a perfect electric conductor plane illuminated by its TEM mode, where r_i and r_e are the inner and outer radii, respectively. In all case studies to be presented, $r_i = 0.45\lambda$ and $r_e = 0.90\lambda$ (see Fig 2).

For the first case study, the main reflector of an omnidirectional ADC configuration was synthesized to radiate, under GO principles, a cosecant square illumination in the elevation plane between $\theta_0 = 115°$ and $\theta_N = 93°$ (Case A.I). As $\theta_0 > \theta_N$, the main reflector has a real caustic (see Fig. 4). The subreflector generating hyperbola was determined from a classical OADC configuration with the following parameters [10]: $V_S = 8.0\lambda$, $D_B = 2.4\lambda$, main-reflector projected diameter $D_M = 17.56\lambda$, focus O at the plane of the main-reflector central opening ($z_B = 0$), main-reflector aperture width $W_A = 7.0\lambda$, and $\gamma = 102°$. These values provide a hyperbola with an eccentricity equal to $\varepsilon = 0.728301$, an inter-focal distance $2c = 42.607\lambda$, and an axis with a tilt angle $\beta = 169.87°$ with respect to the z-axis. As a consequence, the projected diameter of the subreflector $D_S = 18.593\lambda$ and the subreflector edge angle $\theta_E = 58.72°$. In the second example (Case A.II), the subreflector is the same of Case A.I. The main reflector was shaped with an inverted far-field angular limits in the elevation plane (i.e., from $\theta_0 = 93°$ to $\theta_N = 115°$). As $\theta_N > \theta_0$, the main reflector now has a virtual caustic (see Fig. 5). Some relevant dimensions of the shaped antennas of Cases A.I and A.II are listed in Table I.

The shaping procedure discussed in Sect. 2 is simpler than those based on the evaluation of an ordinary differential equation, like that adopted in [7], and it is also simpler than those using general conic sections (ellipses and hyperbolas) [4]–[6]. Regarding the numerical convergence, the present method can provide the same precision of the procedure based on the solution of a differential equation [7] with less steps, but needs more steps than the method based on general conic sections [4]–[6]. To illustrate this, the main-reflector RMS error with respect to a reference

TABLE I
SOME RELEVANT DIMENSIONS OF THE SHAPED ANTENNAS (REF. SOL.)

PARAMET.	*Case A.I*	*Case A.II*
$D_S(\lambda)$	18,593	18,593
$V_S(\lambda)$	8,00	8,00
$D_M(\lambda)$	17,515	17,521
$V_M(\lambda)$	8,566	8,482
$2c(\lambda)$	42,607	42,607
e	0,728301	0,728301
θ_E	58,72º	58,72º
θ_0	115,0º	93,0º
θ_N	93,0º	115,0º
Vol. $10^3\lambda^3$)	4,295	4,275

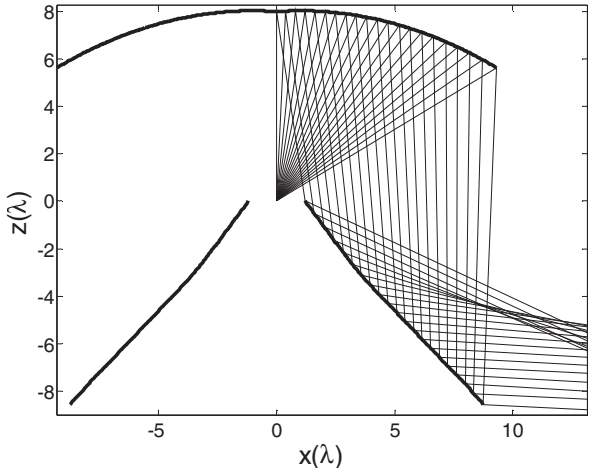

Fig. 4 – Generatrices of a shaped OADC with real caustic

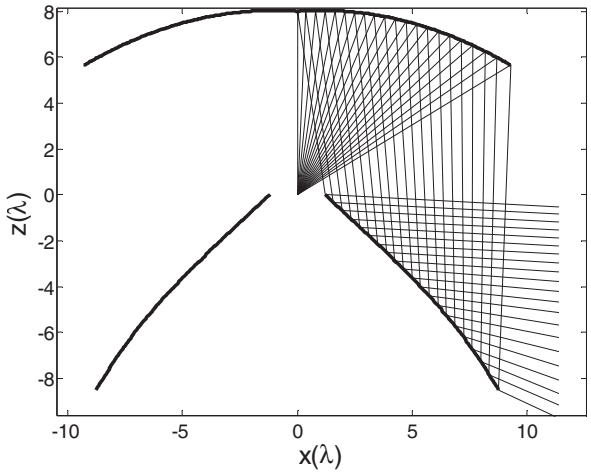

Fig. 5 – Generatrices of a shaped OADC with virtual caustic

reflector shaped with a very large N value are depicted in Fig. 6 as a function of log(1/N) for Cases A.I and A.II.

Figures 7 and 8 show the antenna radiation patterns of Cases A.I and A.II, respectively, simulated by MMT/MoM. Results provided by the three shaping techniques (differential equation, general conic sections, and parabolic conic sections) are presented, all of them with N = 25. The radiation pattern of a configuration shaped with a very large N (reference solution) is also present. As observed, there are small differences between the patterns of the reference solution and that of the method using general conic sections. Although the shaped surfaces obtained from the method discussed here are described by only 25 parabolas, the corresponding radiation patterns show no relevant differences when compared with the reference solutions, unlike the reflectors shaped by the method based on a differential equation with N = 25 [7]. Also, both results (conic and parabolic sections methods) are close to the objective function (6). The small differences observed can be attributed to diffractions effects and electromagnetic coupling not considered by the three GO shaping methods.

Figure 9 shows the return loss obtained from the MMT/MoM analysis for the shaped dual-reflector antennas (Cases A.I and A.II) and for the coaxial TEM horn alone. The differences between the return loss for the antennas (Cases A.I and A.II) and the coaxial TEM horn alone can be mainly attributed to the subreflector backscattering. For this reason the antennas of cases A.I and A.II have approximately the same return loss, since they have the same subreflector, despite having different main reflectors.

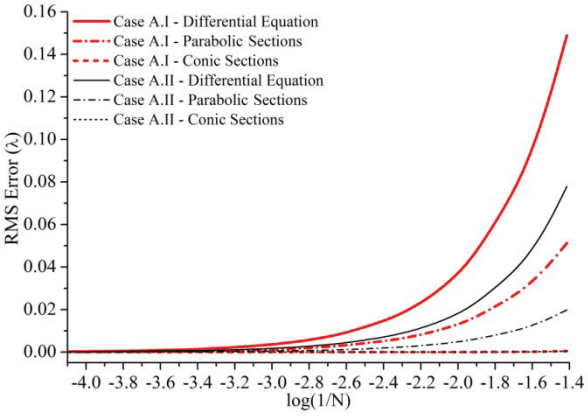

Fig. 6 – Main-reflector RMS error with respect to N for Cases A.I and A.II.

4 CONCLUSIONS

This work presented a method for the GO synthesis of axis-symmetric omnidirectional dual-reflector antennas. The procedure is suited to shape the main-reflector generatrix, which is represented by a series of parabolas consecutively concatenated. The subreflector is not shaped and its generatrix is represented by a single hyperbola section. The main

reflector is designed to offer an omnidirectional coverage with an arbitrary radiation pattern in the vertical plane. Two representative omnidirectional axis-displaced Cassegrainian (OADC) configurations were synthesized, distinguished by the presence of a main-reflector virtual or real caustic.

For both case studies, a full-wave analysis was conducted to validate the shaping procedure and to simulate electromagnetic effects between the coaxial horn and the omnidirectional dual-reflector system. The analysis simulated both the antenna radiation pattern and the return loss inside the coaxial horn.

ACKNOWLEDGMENT

This work was supported in part by CNPq, Brazil, under Projects 470699/2006-0 and 310945/2006-2, and FAPEMIG.

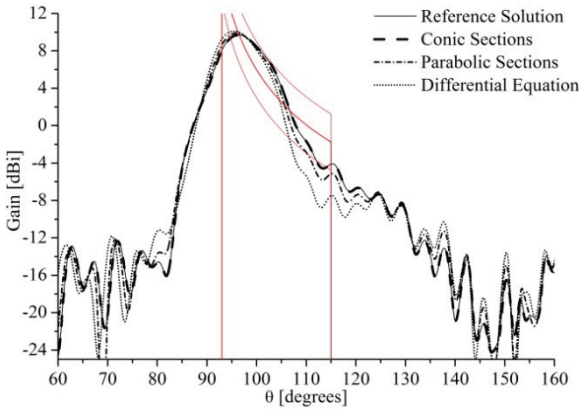

Fig. 7 – MMT/MoM radiation patterns of Case A.I.

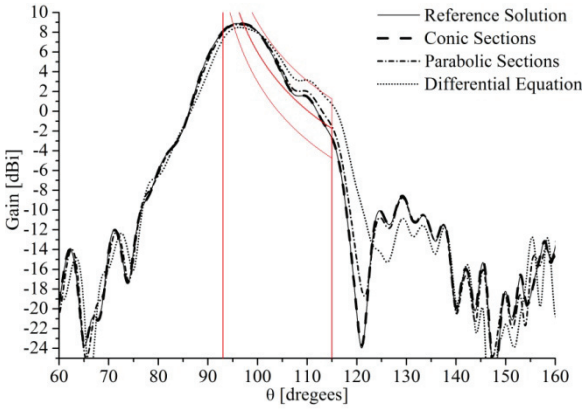

Fig. 8 – MMT/MoM radiation patterns of Case A.II.

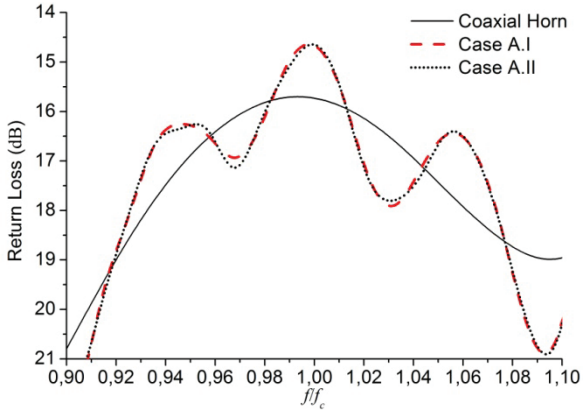

Fig. 9 – MMT/MoM return loss (Cases A.I and A.II).

REFERENCES

[1] Y. Kim and T.-H. Lee, "Shaped Circularly Symmetric dual reflector Antennas by Combining Local Conventional Dual Reflector Systems," IEEE Trans. Antennas Propagat., vol. 57, no 1, pp. 47-56, Jan. 2009.

[2] F. J. S. Moreira and J. R. Bergmann, "Shaping axis-Symmetric Dual-Reflector Antennas by Combining Conic Sections," IEEE Trans. Antennas Propagat., vol. 59, no. 3, pp. 1042-1046, March 2011.

[3] F. J. S. Moreira and J. R. Bergmann, "Omnidirectional dual-reflector shaping by concatenating conic sections," 4th European Conference on Antennas and Propagation (EuCAP 2010), Barcelona, Spain, April 2010.

[4] R. A. Penchel, J. R. Bergmann, and F. Moreira, "An omnidirectional dual-reflector antenna with a shaped main reflector described by local conic sections," 5th European Conference on Antennas and Propagation (EuCAP 2011), Rome, Italy, April 2011.

[5] R. A. Penchel, S. R. Zang, J. R. Bergmann, and F. J. S. Moreira, "Synthesis and Rigorous Analysis of Omnidirectional ADE Antenna with Shaped Main Reflector Described by Local Conic Sections," 6th European Conference on Antennas and Propagation (EuCAP 2012), Prague, Czech Republic, March 2012.

[6] R. A. Penchel, S. R. Zang, J. R. Bergmann, and Fernando J. S. Moreira, "Synthesis and Rigorous Analysis of Omnidirectional Dual-Reflector Antennas with Shaped Main Reflector Described by Local Conic Sections," 7th Loughborough Antennas & Propagation Conference (LAPC 2011), Loughborough, U.K., November 2011.

[7] J. R. Bergmann and F. J. S. Moreira, "Omnidirectional ADE antenna with GO shaped main reflector for arbitrary far-field pattern in the elevation plane," IET Microwaves, Antennas & Propagation, vol. 3, no. 5, pp. 1028-1035, Oct. 2009.

[8] E. Kuhn and V. Hombach, "Computer-aided analysis of corrugated horns with axial or ring-loaded radial slots", Proc. ICAP 83, Part 1, pp.127-131, 1983.

[9] K. Lui, C. Balanis, C. Birtcher, and G. Barber, "Analysis of pyramidal horn antennas using moment methods", *IEEE Trans. Antennas Propagat.*, vol. 41, no. 10, pp. 1379–1389, Oct. 1993.

[10] F. J. S. Moreira and J. R. Bergmann, "Axis-Displaced Dual-Reflector Antennas for Omnidirectional Coverage with Arbitrary Main-Beam Direction in the Elevation Plane," IEEE Transactions on Antennas and Propagation, vol. 54, no. 10, pp. 2854—2861, Oct. 2006.